A TISSUE-ENGINEERED NEURAL INTERFACE WITH PHOTOTHERMAL FUNCTIONALITY

Adriana Teixeira do Nascimento[1,2], Alexandre Xavier Mendes[1,2], James M. Begeng[1,3], Serena Duchi[2,4], Paul R. Stoddart[5], Anita F. Quigley[2,7,8], Robert M. I. Kapsa[2,7,8]; Michael R. Ibbotson[3,9], Saimon M. Silva[1,2,6*], Simon E. Moulton [1,2,6*]

[1] ARC Centre of Excellence for Electromaterials Science, School of Science, Computing and Engineering Technologies, Swinburne University of Technology, Melbourne, Victoria 3122, Australia

[2] The Aikenhead Centre for Medical Discovery, St Vincent's Hospital Melbourne, Melbourne, Victoria 3065, Australia

[3] National Vision Research Institute, The Australian College of Optometry, Carlton, VIC 3058, Australia

[4] Department of Surgery, University of Melbourne, St Vincent's Hospital, Melbourne, Victoria 3065, Australia

[5] School of Science, Computing and Engineering Technologies, Swinburne University of Technology, Hawthorn, Victoria 3122, Australia

[6] Iverson Health Innovation Research Institute, Swinburne University of Technology, Melbourne, Victoria 3122, Australia

[7] School of Electrical and Biomedical Engineering, RMIT University, Melbourne, Victoria 3001, Australia

[8] Department of Medicine, University of Melbourne, St Vincent's Hospital Melbourne, Victoria 3065, Australia

[9] Department of Optometry and Vision Sciences, University of Melbourne, Parkville, Victoria 3010, Australia

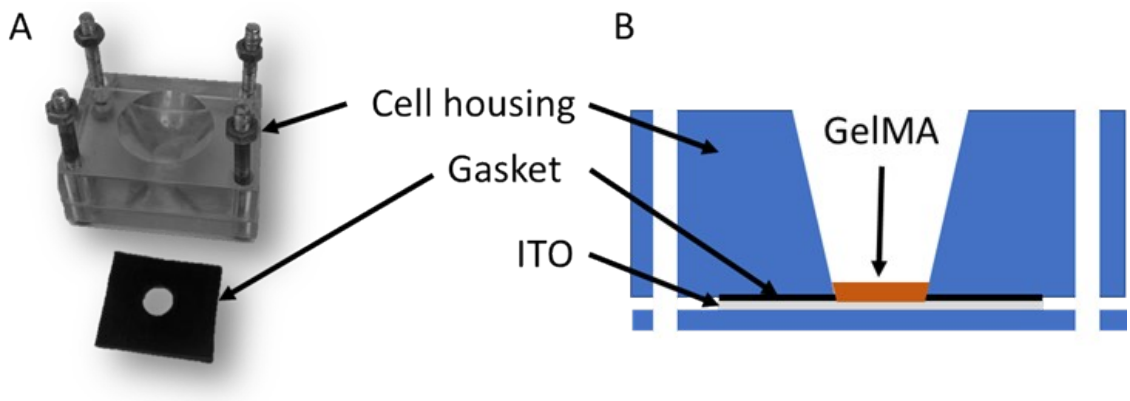

Figure S1 - Electrochemical cell designed for the electrochemical investigations.

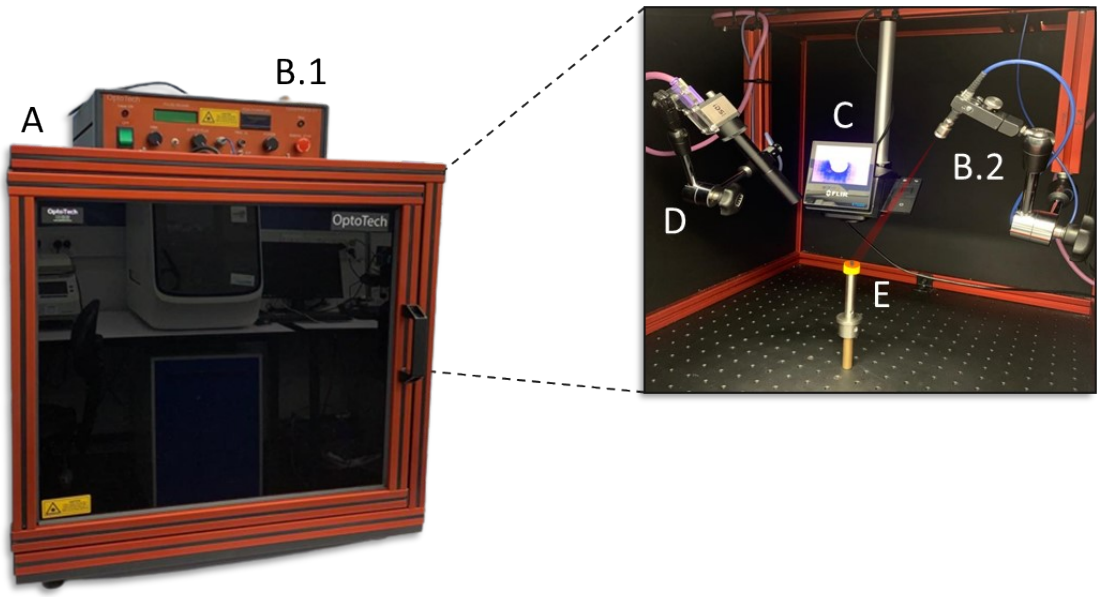

Figure S2 - Laser instrumentation setup used for the NIR Optical Stimulation containing: A) Biosafety cabinet, B.1) Laser system; B.2) Optic fibre end; C) Thermal camera; D) Visible camera; and E) Scaffold standing platform.

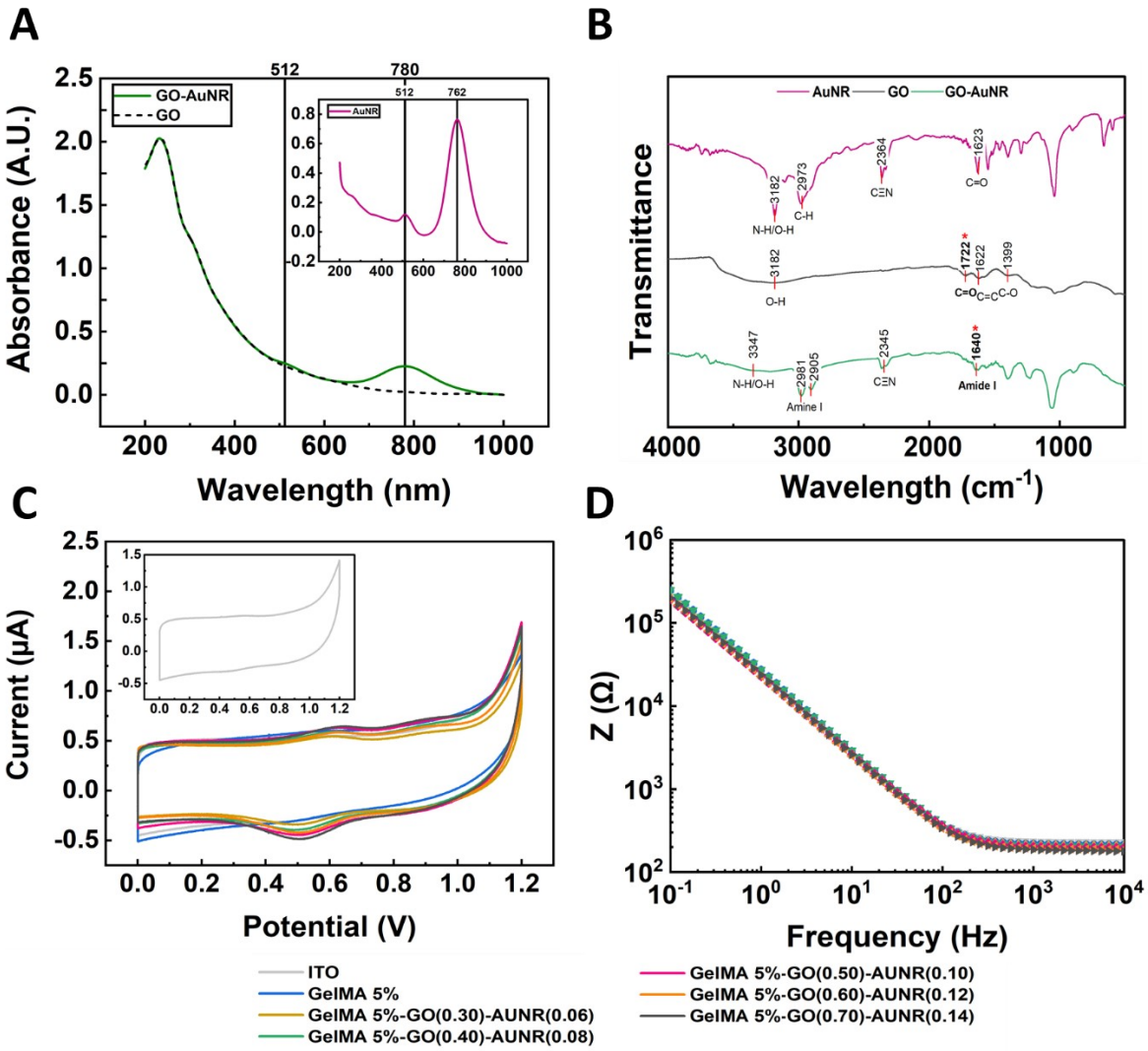

Figure S3 - Material characterisation presenting the confirmation of composite functionalisation through the EDC/Sulfo-NHS covalent conjugation in the UV-vis spectra for the wavelength range 200-1000 nm. A) Composite binding confirmation through the comparison of the UV-vis spectra of both GO (1.25 mg.mL^{-1}) and GO-AuNRs (1.25: 0.25 mg.mL^{-1}) showing its photoactivity in the NIR range by the presence of the SPR peak ≈ 512 nm and LSPR peak ≈ 762 nm (inset spectrum). B) FTIR spectra of AuNRs (protein-A coated), GO (1.25 mg.mL^{-1}), and GO-AuNRs (1.25; 0.25 mg.mL^{-1}) for the wavenumber range of 600-4000 cm^{-1}, performed to further confirm the composite functionalisation of the hydrogel. C) Cyclic voltammetry (CV) electrochemical characterisation with the potential range from 0 to 1.2V and scan rate 0.05 V/s, highlighting the electroactivity of the composite within the hydrogel by presenting redox peaks around ≈ +0.6 V (oxidation) and ≈ -0.5 V (reduction). D) Bode plot presenting the impedance of the composites at a range of concentration in mg.mL^{-1}.

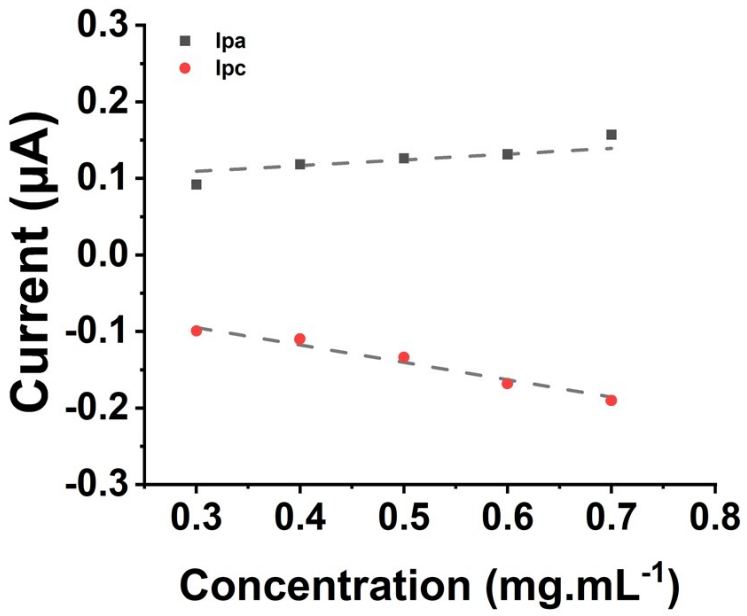

Figure S4 - Dependence of the current peak (Ipa and Ipc) versus the concentration of the composite in $mg.mL^{-1}$ extracted from the CV (Figure 1C) presenting the linear behaviour of the samples indicating that the redox reaction is reversible.

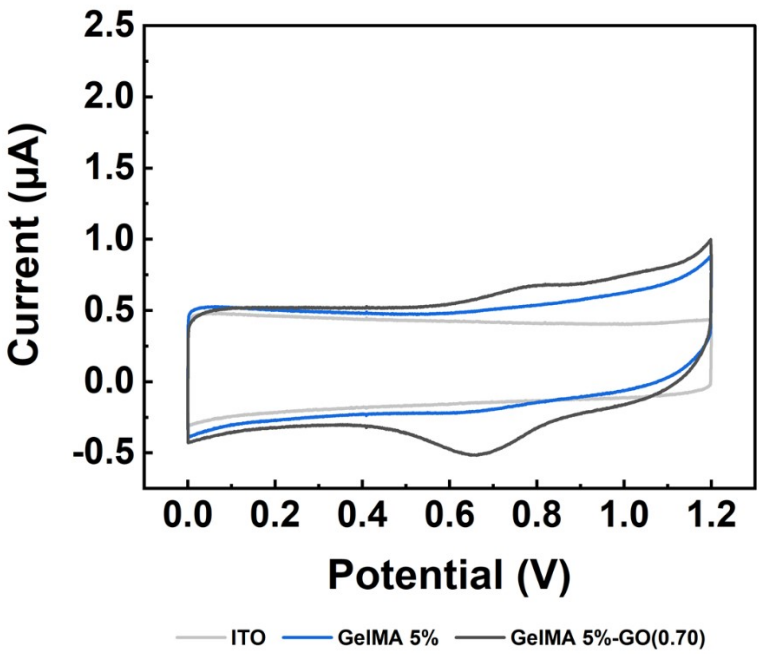

Figure S5 - Cyclic voltammogram recorded between 0 to 1.2 V at a scan rate 0.05 V/s, highlighting the electroactivity of GO within the hydrogel by presenting redox peaks around ≈ + 0.75 V (oxidation) and ≈ - 0.65 V (reduction).

The impedance values measured at 3 frequencies from the Bode plot (Figure S3D) are presented in Table S1.

Table S1 - EIS investigation presenting the decrease in the current inversely proportional to the increase in the concentration in $mg.mL^{-1}$ at higher frequencies.

Samples	**Concentrations ($mg.mL^{-1}$)***	**Z (Ω) x 10^2**		
		$3x10^2$ Hz	**1 kHz**	**3kHz**
GelMA	5% w/v	2.5	2.3	2.2
GelMA-GO-AuNR	0.30-0.06	2.4	2.2	2.1
	0.40-0.08	2.3	2.1	2.1
	0.50-0.10	2.3	2.1	2.0
	0.60-0.12	2.1	1.1	1.9
	0.70-0.14	2.1	1.9	1.8

*The first and second concentration value for the GelMA-GO-AuNR samples is the GO and AuNR respectively.

Table S2 - Summary of mechanical characterisation results extracted from the data presented in Figure 1.

Samples	**Concentrations**	**Units**	**Storage modulus (kPa)**	**Crosslinking rate (s)**	**Yong's modulus (kPa)**	**Swelling ratio**
GelMA	5%	w/v	0.3 ± 0.13	270 ± 0.04	3 ± 0.10	18 ± 0.03
GelMA-GO	0.30	$mg.mL^{-1}$	0.6 ± 0.07	308 ± 0.04	3 ± 0.07	14 ± 0.04
	0.50		0.7 ± 0.01	282 ± 0.03	4 ± 0.05	13 ± 0.02
	0.70		0.8 ± 0.04	286 ± 0.04	4 ± 0.07	11 ± 0.05
GelMA-GO-AuNRs	0.30-0.06		0.6 ± 0.05	312 ± 0.03	3 ± 0.07	13 ± 0.02

	0.50-0.10		0.8 ± 0.05	322 ± 0.02	4 ± 0.07	12 ± 0.05
	0.70-0.14		0.2 ± 0.04	305 ± 0.04	4 ± 0.02	12 ± 0.02

*The first and second concentration value for the GelMA-GO-AuNR samples is the GO and AuNR respectively.

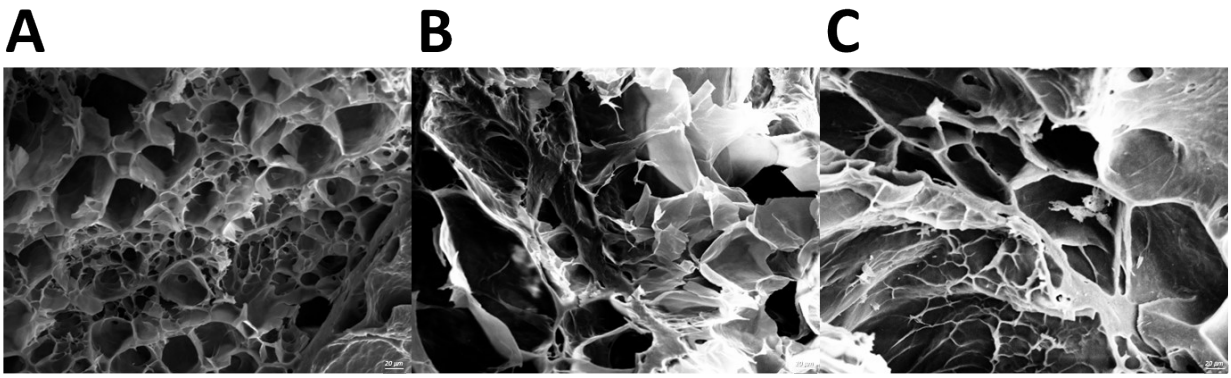

Figure S6 – SEM pictures presenting the morphology for the cross-section of the scaffolds. A) GelMA, B) GelMA-GO and C) GelMA-GO-AuNR.